A New Approach to Vessel Enhancement in Angiography Images

Phan Tran Ho Truc[1], Mohammad A. U. Khan[2], Sungyoung Lee[1], and Tae-Seong Kim[3]

[1]Department of Computer Engineering, Kyung Hee University, Suwon, South Korea, 446-701,
[2]Comsats Institute of Information Technology, Abbottabad, Pakistan,
[3]Department of Biomedical Engineering, Kyung Hee University, Suwon, South Korea, 446-701.

***Abstract*— Conventional vessel enhancement approaches used in literature are Hessian-based filters, which are sensitive to noise and sometimes give discontinued vessels due to junction suppression. In this paper, we propose a new approach incorporating the use of linear directional features of vessels to get more precise estimates of the Hessian eigenvalues in noisy environment. The directional features are extracted from a set of directional images which are obtained by decomposing the input image using a Directional Filter Bank. In addition, the directional image decomposition helps to avoid junction suppression, which in turn, yields continuous vessel tree. Experimental results show that the proposed filter generates better performance in comparison against conventional Hessian-based approaches.**

I. Introduction

Vessel enhancement procedure is an important preprocessing step in automatic vessel-tree reconstruction which is critical to a number of clinical procedures, but has proven to be a challenging task, especially with angiography images. The key fact is that vessels cannot be characterized uniformly: arteries, or big vessels, usually have high contrast while small ones resemble the background, as can be seen in Fig. 4(a). In literature, there are many vessel enhancement methods. The simplest one is to threshold the raw data but this makes the segmentation process incorrectly label bright noise regions as vessels and cannot recover small vessels which may not appear connected in the image. Recently, Hessian-based approaches have been utilized in numerous vessel enhancement filters [1], [2], [3], and [4]. These filters are based on the principal curvatures, which are determined by the Hessian eigenvalues, to differentiate the line-like (vessel) from the blob-like (background) structures. Fig. 1 provides the block diagram of the procedures commonly employed in these conventional approaches. However, their main disadvantage is that they are highly sensitive to noise due to second-order derivatives and sometimes give discontinued vessels due to junction suppression [5].

In this paper, we propose a new framework for the vessel enhancement utilizing the linear directional information present in a set of directional images which are obtained by decomposing the input image using an appropriate Directional Filter Bank. The directional decomposition has two advantages. One is, noise in each directional image will be significantly reduced compared to that in the original one due to its omni-directional nature. The second is, because one directional image contains vessels with similar directions, the principal curvature calculation in it is facilitated. After obtaining directional images, appropriate vessel enhancement filters are applied and the enhanced directional images are re-combined to generate the output image with enhanced vessels and suppressed noise. This decomposition-filtering-recombination scheme also helps to preserve junctions. The experimental results show that our approach is less noise sensitive and avoid junction suppression.

II. Methodology

The proposed framework consists of four steps, as shown in Fig. 2: Step 1) construction of directional images, Step 2) vessel axis aligning, Step 3) vessel enhancement, and Step 4) recombination of enhanced directional images.

A. Construction of Directional Images

Directional Filter Bank and Decimation-Free Directional Filter Bank: Directional Filter Bank (DFB) was originally proposed by Bamberger and Smith [6] and then improved by Park, Smith and Mersereau [7], [8]. It was shown that DFB can decompose the spectral region of an input image into wedge-shaped like passbands which correspond to linear features in a specific direction in spatial domain. Outputs of DFB are named as subbands whose sizes are smaller than that of the input image. The reduction in size is due to the presence of decimators. As far as image compression is concerned, decimation is a must condition. But whenever DFB is employed for image analysis purposes, decimation causes two problems. One is, as we increase the directional resolution, spatial resolution starts to decrease [9], due to which we loose the correspondence among the pixels of DFB outputs. The other is, an extra process of interpolation is involved prior to enhancement or recognition algorithm implementation [10], [11]. This extra interpolation process does not only affect the efficiency of whole system but also produces false artifacts which can be harmful especially in case of medical imagery. Some vessels may be broken and some can be falsely connected to some other vessels due to the artifacts produced by interpolation. So a need arises to modify directional filter bank structure in the sense that no decimation is required during analysis section. To meet that need, the authors in [12] and [7] presented new rules to modify DFB. Based on those rules, we suggest to shift the decimators

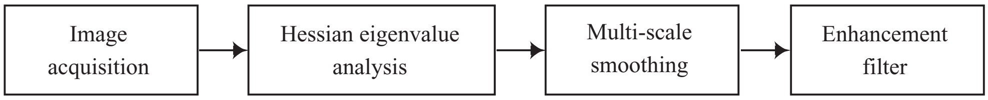

Fig. 1. Block diagrams of conventional Hessian-based approaches.

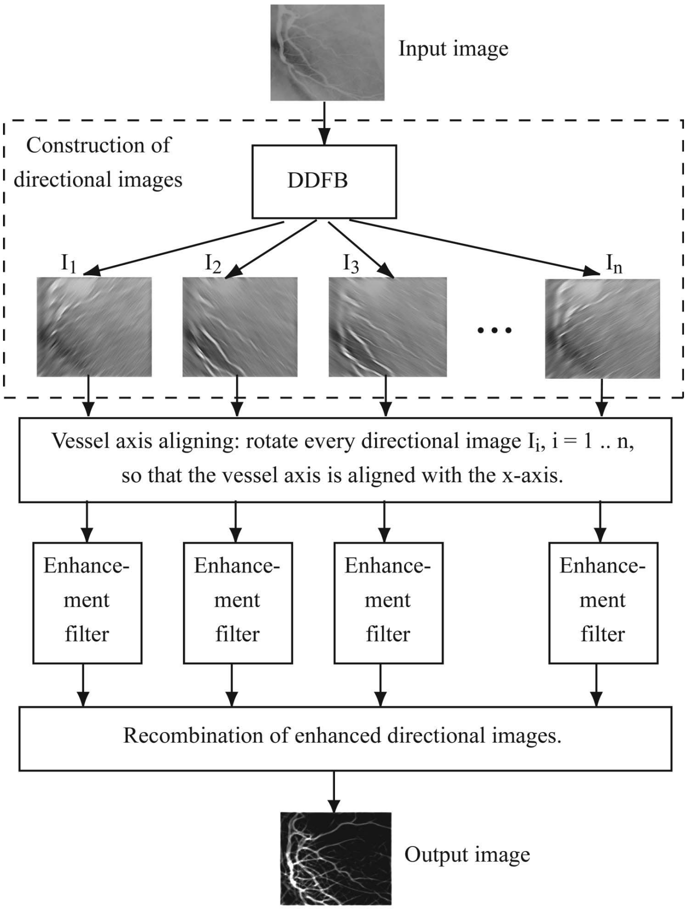

Fig. 2. Block diagram of the proposed enhancement framework. There are four main steps: construction of directional images, vessel axis aligning, vessel enhancement, and recombination of enhanced directional images.

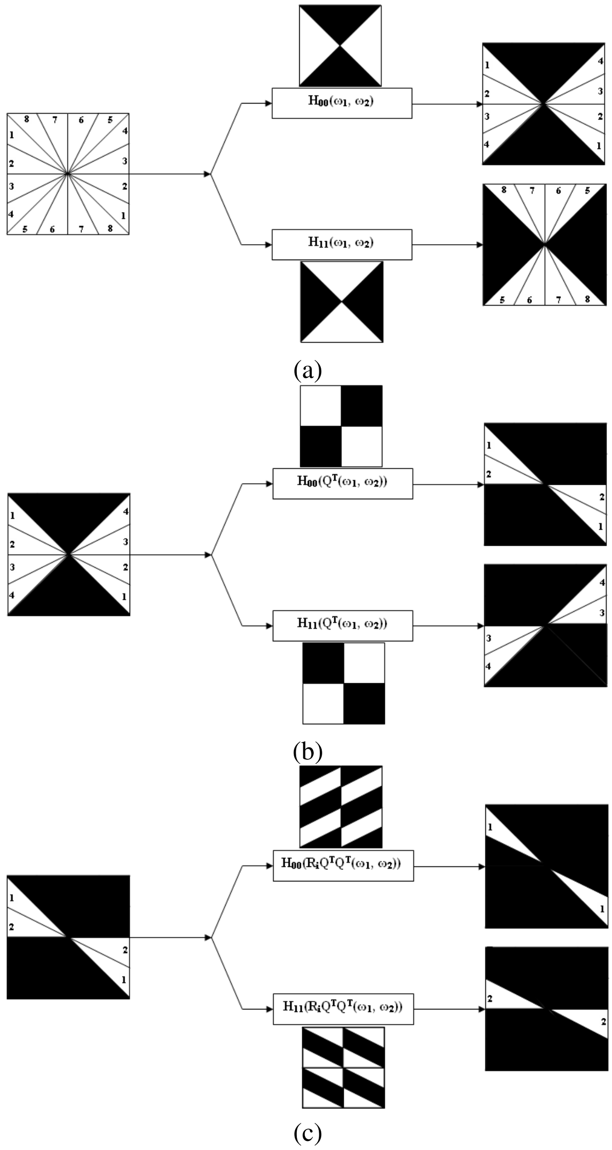

Fig. 3. DDFB structure a) First stage b) Second stage c) Third stage, where $H_{00}(\omega_1, \omega_2)$ and $H_{11}(\omega_1, \omega_2)$ are hourglass-shaped like passbands, Q and R_i are respectively downsampling and resampling matrices as in [7], [8].

and resamplers to the right of the filters to make a *Decimation-free Directional Filter Bank* (DDFB), which yields *directional images* rather than directional subbands. This consequently results in elimination of interpolation and naturally fits the purposes of feature analysis. The block diagram of the DDFB structure is shown in Fig. 3. In this diagram, $H_{00}(\omega_1, \omega_2)$ and $H_{11}(\omega_1, \omega_2)$ are hourglass-shaped like passbands, Q is a Quincunx downsampling matrix, and R_i's are resampling matrices as used in [7], [8].

In Step 1 of our framework, the input image is decomposed to $n = 2^k$ $(k = 1, 2, ...)$ directional images I_i using DDFB. The motivation here is to detect thin and low-contrast vessels (which are largely directional in nature) while avoiding false detection of non-vascular structures. Directional segregation property of DDFB is helpful in eliminating randomly oriented

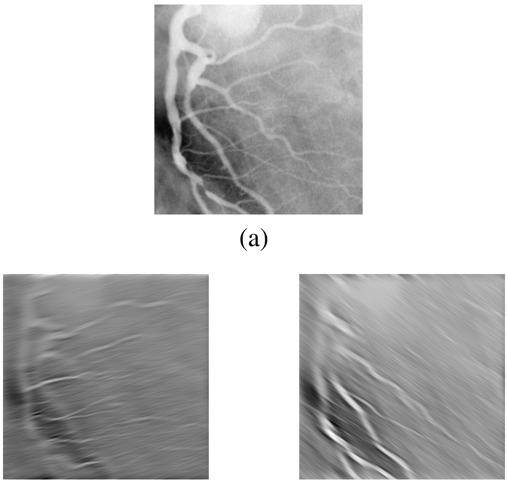

(a)

(b) (c)

Fig. 4. Two demonstrative directional images obtained by DDFB with $k = 3$. (a) Input image, (b) Directional image corresponds to orientations in the range 0-22.5 degree, and (c) 135-157.5 degree.

noise patterns and non-vascular structures which normally yield similar amplitudes in all directional images. Two out of eight ($n = 8$ or $k = 3$) resulting directional images of DDFB are demonstratively shown in Fig. 4. All those images are then aligned in the following step.

B. Vessel Axis Aligning

An intensity image $I(p)$, where $p = (x, y)$, can be approximated by its Taylor expansion about a point p_0 up to the second order:

$$I(p) \simeq I(p_0) + \Delta p^T \cdot \nabla I(p_0) + \frac{1}{2}\Delta p^T H(I(p_0))\Delta p \quad (1)$$

$$\Delta p = p - p_0 \quad (2)$$

where $\nabla I(p_0)$ and $H(I(p_0))$ are respectively the gradient vector and the Hessian matrix at point p_0.

In angiography images, vessels are bright over the dark background and the brightness is decreased from their centers toward their boundaries. Therefore, a vessel is modeled as a tube with a Gaussian profile across its axis, which is identical to the x-axis:

$$I_0(x, y) = \frac{C}{2\pi\sigma_0^2} e^{-\frac{y^2}{2\sigma_0^2}}. \quad (3)$$

The Hessian can then be expressed as:

$$H = \begin{bmatrix} \frac{\partial^2 I_0}{\partial x^2} & \frac{\partial^2 I_0}{\partial x \partial y} \\ \frac{\partial^2 I_0}{\partial x \partial y} & \frac{\partial^2 I_0}{\partial y^2} \end{bmatrix} = \begin{bmatrix} 0 & 0 \\ 0 & \frac{y^2 - \sigma_0^2}{\sigma_0^4} I_0 \end{bmatrix} \quad (4)$$

and its eigenvalues and eigenvectors:

$$\begin{array}{l|l} \lambda_1 = 0 & \lambda_2 = \frac{y^2 - \sigma_0^2}{\sigma_0^4} I_0 \\ \vec{v_1} = (1, 0) & \vec{v_2} = (0, 1). \end{array} \quad (5)$$

In order to capture vessels with various sizes, one should compute the gradient and the Hessian at multiple scales σ in a certain range. In this case, the only way to ensure the well-posed properties, such as linearity, translation invariance, rotation invariance, and re-scaling invariance, is the use of linear scale space theory [13], [14], in which differentiation is calculated by a convolution with derivatives of a Gaussian:

$$I_x = \sigma^\gamma G_{x,\sigma} * I \ ; \ I_y = \sigma^\gamma G_{y,\sigma} * I \quad (6)$$

where $I_x, I_y, G_{x,\sigma}$ and $G_{y,\sigma}$ are respectively the spatial derivatives in x- and y- direction of the image $I(x, y)$ and of a Gaussian with standard deviation σ:

$$G_\sigma(x, y) = \frac{1}{2\pi\sigma^2} e^{-\frac{x^2+y^2}{2\sigma^2}}. \quad (7)$$

The parameter γ was proposed by Lindeberg [14], [15] to normalize the derivatives of the image. This normalization is necessary for comparison of the response of differentiations at multiple scales because the intensity and its derivatives are decreasing functions of scale. In vessel enhancement application, where no scale is preferred, γ is usually set to one.

When applying the multiscale analysis, the model in (3) is convolved with a Gaussian of standard deviation σ. The derivations in (4) and (5) are still correct except that σ_0 is replaced with $\sqrt{\sigma_0^2 + \sigma^2}$. We can see from those derivations that, when the vessel direction ($\vec{v_1}$) is aligned with the x-axis, eigenvalues of the Hessian are same as its diagonal values. Exploiting this fact, we can compute the principal curvatures with less noise sensitiveness compared to the normal way. To do so, the directional images I_i's obtained from the previous step are rotated such that the vessel axis is aligned with the x-axis.

Suppose the directional image I_i corresponds to the orientations ranging from α^i_{min} to α^i_{max} (counterclockwise). It will be rotated by an amount as large as the mean value m^i_α:

$$m^i_\alpha = \frac{\alpha^i_{min} + \alpha^i_{max}}{2}. \quad (8)$$

Let I'_i denote the aligned directional images. Then

$$I'_i = rotate(I_i, m^i_\alpha) \quad (9)$$

where $i = 1, 2, ..., n$, and n is the total number of directional images.

C. Vessel Enhancement

In this step, every aligned directional image is filtered by an appropriate vessel enhancement filter. Because the directions of vessels in these directional images are now aligned with the x-axis, the proposed enhancement filter utilizes the diagonal values of the Hessian matrix instead of its eigenvalues, as proven in (3)$-$(5). These values are:

$$h_{11} = 0; \quad h_{22} = \frac{y^2 - (\sigma_0^2 + \sigma^2)}{(\sigma_0^2 + \sigma^2)^2} I_0(x, y) \quad (10)$$

where σ selected in a range S is the standard deviation of the Gaussian kernel used in multiscale analysis.

Practically, the vessel axis is not, in general, identical to the $x-$axis and so $h_{11} \approx 0$. Inside the vessel, $|y| < \sqrt{\sigma_0^2 + \sigma^2}$

and thus h_{22} is negative. Therefore, vessel pixels are declared when $h_{22} < 0$ and $\left|\frac{h_{11}}{h_{22}}\right| << 1$.

To distinguish background pixels from others, we define a structureness measurement which is similar to the "second-order structureness" defined in [1]:

$$C = \sqrt{h_{11}^2 + h_{22}^2}. \tag{11}$$

This structureness C should be low for background which has no structure and small derivative magnitude.

Based on the above observations, the vessel filter output can be defined as

$$\phi_\sigma(p) = \eta(h_{22})exp\left(-\frac{R^2}{2\beta^2}\right)\left[1 - exp\left(-\frac{C^2}{2\gamma^2}\right)\right] \tag{12}$$

where $p = (x, y)$, $R = \frac{h_{11}}{h_{22}}$, β and γ are adjusting constants, and

$$\eta(z) = \begin{cases} 0 & \text{if } z \geq 0; \\ 1 & \text{if } z < 0. \end{cases} \tag{13}$$

The filter is analyzed at different scales σ in a range S. When the scale matches the size of the vessel, the filter response will be maximum. Therefore, the final vessel filter response is:

$$\Phi(p) = \max_{\sigma \in S} \phi_\sigma(p). \tag{14}$$

One filter (14) is applied to one directional image to enhance vessel structures in it. Then all enhanced directional images are re-combined to generate the final result.

D. Recombination of Enhanced Directional Images

Each directional image now contains enhanced vessels in its directional range and is called the enhanced directional image.

Denote $\Phi_i(p), i = 1..n$, as the enhanced directional images. These images need rotating back to their original orientations:

$$\Phi_i'(p) = rotate(\Phi_i(p), -m_\alpha^i) \tag{15}$$

where m_α^i is given in (8).

The output enhanced image $F(p)$ can be obtained by

$$F(p) = \frac{1}{n}\sum_{i=1}^{n} \Phi_i'(p). \tag{16}$$

The whole filtering procedures can be summarized as follows. First, the input angiography image is decomposed into $n = 2^k$ $(k = 1, 2, ...)$ directional images I_i using DDFB. Then, every directional image I_i is rotated based on (9). Next, the rotated directional images I_i' are enhanced according to (12)−(14). Finally, all enhanced images are rotated back using (15) and re-combined to yield the final filtered image F as in (16).

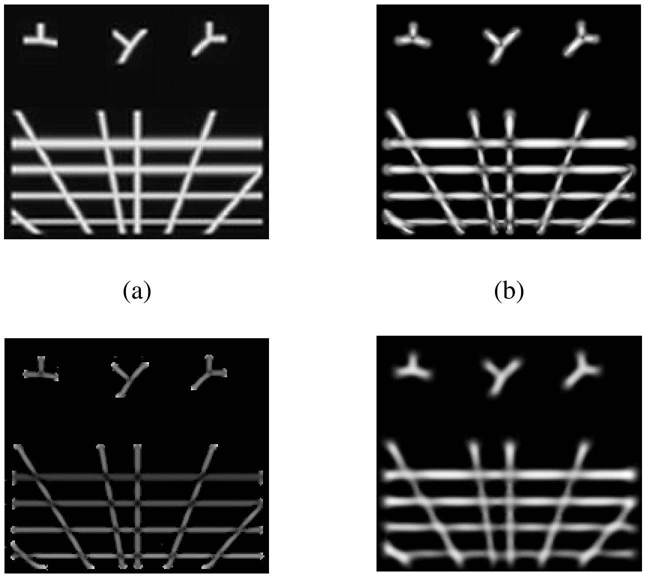

(a) (b) (c) (d)

Fig. 5. Vessel enhancement results. (a) The original synthetic image. (b) Enhanced image by Frangi method, (c) by Shikata method, and (d) by our approach. The Frangi and Shikata models unexpectedly suppress the junctions while ours does not.

III. Experimental Results

In this section, experiments have been performed with both synthetic images and real angiography images to verify the performance of the proposed enhancement filter in comparison with the filters introduced by Frangi [1] and Shikata [4], which are considered as the standard techniques. In experiments using our proposed filter, the input image is decomposed to sixteen directional images ($k = 4$) as a trade-off between performance and execution time. The scale range $S = \{1, \sqrt{2}, 2, 2\sqrt{2}, 4\}$ is used for all three models as proposed in [4] .

A. Junction Suppression

Fig. 5 shows the results of an synthetic image which was processed by the three filter models. The synthetic image is designed to contain vessels of different sizes and junctions of different types. It is possible to see that the Frangi and Shikata filters unexpectedly suppress junctions while our proposed approach does not. The suppressed junctions make vessels discontinuous. Although this error may be small, it can cause the splitting of a single vessel, which in turn has a critical effect on the vessel-tree reconstruction accuracy.

It is the use of directional image decomposition that makes the proposed model work. Normally, a vessel has one principal direction, which is mathematically indicated by a small ratio between the smaller and larger Hessian eigenvalue. Meanwhile, at a junction, where a vessel branches off, there are more than two principal directions, and thus the ratio of two eigenvalues is no longer small. As a result, the conventional enhancement filters [1], [4] consider those points as noise and then suppress them. Our proposed approach, on the other hand, decomposes the input image to various directional images, each of which contains vessels with similar orientations. Consequently, junctions do not exist in directional images and so are not suppressed during the filtering process. After that, due to the re-combination of enhanced directional images, junctions are re-constructed at those points which have vessel values in more than two directional images. Therefore, junctions are not only preserved but also enhanced in the final output image.

B. Simulation Study - A Quantitative Evaluation

To evaluate our approach, mathematical models of phantoms were constructed. First of all, one original phantom image with various typical enhancement hindrances such as the diversity in vessel orientations and widths, the presence of close parallel vessels, very thin vessels, discontinued vessels, and vessels with variable intensities along their length, etc. was created. This original phantom image is used as the "ground truth". Then, a set of testing images were generated from the original phantom by adding various levels of white noise, having variance from 5% to 80%. The noise variance is calculated as a percentage of the 8-bit dynamic range of the image (0-255). The 80%-noise variance image was selected to explore the enhancement performance for the *worst case*. It means that, to our experience, this image represents the most possibly challenging situation, which is well beyond any worst case of real angiography images.

In this experiment, every sample image in the testing dataset was first processed by each of the three enhancement algorithms (Frangi filter, Shikata filter, and our DFB-based filter). The results were then segmented by using an adaptive global threshold as follows. Let the *vessel ratio* of an image be the ratio between the number of vessel-labeled pixels and the total number of pixels in that image. Then, for each filtered image, the global threshold value is chosen so that its *vessel ratio* is as close to that of the "ground truth", which is approximately 11% in this case, as possible. Finally, a "goodness" measurement is used to quantitatively evaluate the filters' performances.

There are many kinds of performance measurement that are not uniquely defined in the literature. In this paper, the *accuracy* definition introduced in [16] is adopted:

$$accuracy = \frac{TP + TN}{TP + FP + TN + FN} \,. \tag{17}$$

Here, vessel-labeled pixels are considered positive and background pixels negative. TP denotes the number of true positive pixels (correctly classified as vessels) compared with the "ground truth", TN true negative (correctly classified as background), FP false positive (background misclassified as vessels), and FN false negative (vessels misclassified as background).

Fig. 6 shows the enhancement results for one sample data having noise variance 10% using the three enhancement algorithms. Visually, the proposed filter gives better enhancement results. The performances of these algorithms applied on the whole testing data are presented in Fig. 7. In this figure, the

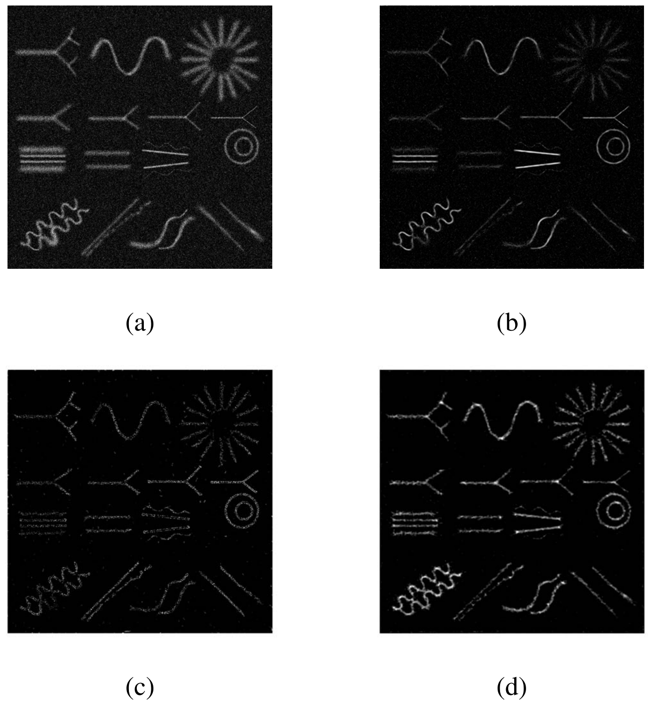

Fig. 6. Sample enhancement results. (a) Sample phantom image with noise variance 10%. (b) Enhanced image by Frangi filter, (c) by Shikata filter, and (d) by our approach. Visually, the proposed filter gives better enhancement results.

accuracy measurements are plotted as a function of the noise variance. It is clear that the our approach outperformed the others for this dataset.

C. Real Data

Similar to junction suppression problem, small vessel enhancement is critical because those thin vessels which may appear broken or disconnected from larger structures will often be omitted in reconstruction procedures. The major fact which prevents small vessels from being easily enhanced is that small vessels usually have low intensity and thus resemble background.

Fig. 8 shows our approach enhancement results (right column) together with the results acquired using Frangi (middle left) and Shikata (middle right) filters for the input images shown in the left column. As can be observed, Frangi filter gives good results with large vessels but fails to detect small ones while Shikata model is able to enhance small vessels but unfortunately enhances background noise also. Conversely, our proposed filter can enhance small vessels with more continuous appearances.

IV. Conclusion

We have presented in this paper a novel approach for vessel enhancement in angiography images. The approach utilizes the image directional information obtained by the *decimation-free directional filter bank* to provide a relief for Hessian analysis in noisy environment. In addition, the fact that enhancement filters are applied not on the original image but on the directional

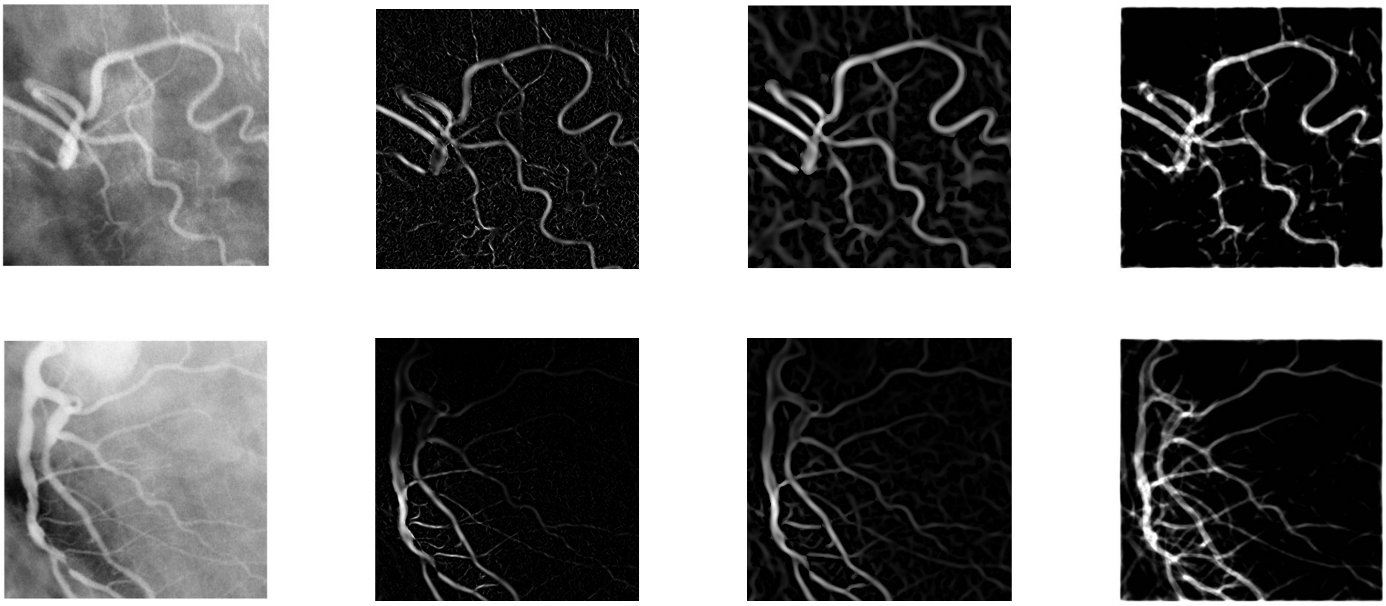

Fig. 8. Vessel enhancement in actual angiography images. LEFT columm: Original images, MIDDLE LEFT column: Enhanced images by Frangi method, MIDDLE RIGHT columm: by Shikata method, and RIGHT column: by our approach. The Frangi and Shikata models fail to correctly enhance small vessels but our approach succeeds.

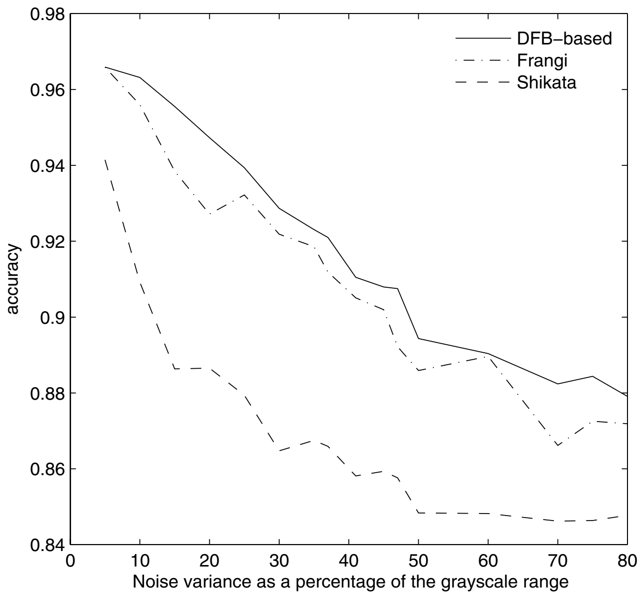

Fig. 7. Vessel enhancement performance of our proposed filter, Frangi filter, and Shikata filter as a function of noise variance. The noise variance is calculated as the percentage of the grayscale range (0-255). The proposed filter gives the best results for this dataset.

ones, which contains vessels in similar orientations, helps to avoid unexpected junction suppression. Consequently, as shown in the experiment results, the proposed filter overcomes limitations of conventional Hessian-based methods such as the noise sensitivity, junction suppression, and limited small vessel enhancement. In conclusion, we consider it a suitable candidate for a pre-processing step in an accurate vessel-tree reconstruction in clinical tasks.

ACKNOWLEDGMENT

This research was supported by the MIC (Ministry of Information and Communication), Korea, under the ITRC (Information Technology Research Center) support program supervised by the IITA (Institute of Information Technology Advancement) (IITA-2006-C1090-0602-0002).

This work was supported by a grant of Korea Health 21 R&D Project, Ministry of Health and Welfare, Republic of Korea (02-PJ3-PG6-EV07-0002).

REFERENCES

[1] A.F. Frangi, W.J. Niessen, K.L. Vincken, and M.A. Viergever, "Multiscale vessel enhancement filtering," *Proc. Int. Conf. Medical Image Computing Computer-Assisted Intervention, LNCS*, vol. 1496, pp. 130–137, 1998.

[2] Y. Sato, S. Nakajima, N. Shiraga, H. Atsumi, S. Yoshida, T. Koller, G. Gerig, and R. Kikinis, "Three-dimensional multi-scale line filter for segmentation and visualization of curvilinear structures in medical images," *Medical Image Analysis*, vol. 2, no. 2, pp. 143–168, 1998.

[3] C. Lorenz, I.-C. Carlsen, T.M. Buzug, C. Fassnacht, and J. Weese, "A multi-scale line filter with automatic scale selection based on the Hessian matrix for medical image segmentation," *Proc. Scale-Space Theories in Computer Vision, LNCS*, vol. 1252, pp. 152–163, 1997.

[4] H. Shikata, E. A. Hoffman, and M. Sonka, "Automated segmentation of pulmonary vascular tree from 3D CT images," in *Proc. SPIE Int. Symp. Medical Imaging*, San Diego, CA, 2004.

[5] G. Agam, III S.G. Armato, and C. Wu, "Vessel tree reconstruction in thoracic CT scans with application to nodule detection," *IEEE Trans. Med. Imag.*, vol. 24, no. 4, pp. 486–499, Apr. 2005.

[6] G.H. Bamberger and M. J. T. Smith, "A filter bank for the directional decomposition of images - theory and design," *IEEE Trans. Sig. Proc.*, vol. 40, no. 4, pp. 882–893, 1992.

[7] S. Park, M. J. T. Smith, and R. M. Mersereau, "A new directional filter bank for image analysis and classification," *ICASSP*, vol. 3, pp. 1417–1420, 1999.

[8] S. Park, M. J. T. Smith, and R. M. Mersereau, "Improved structures of maximally decimated directional filter banks for spatial image analysis," *IEEE Trans. Image Processing*, vol. 13, no. 11, pp. 1424–1431, Nov. 2004.

[9] R. H. Bamberger, *The directional filter bank: A multirate filterbank for the directional decomposition of images*, Ph.D. thesis, Georgia Institute of Technology, Nov. 1990.

[10] R. H. Bamberger, "New results on two and three dimensional directional filter banks," in *IEEE Twenty-Seventh Asilomar Conference on Signals, Systems and Computers*, Nov. 1993, vol. 2, pp. 1286–1290.

[11] R. H. Bamberger and M. J. T. Smith, "A multirate filter bank based approach to the detection and enhancement of linear features in images," in *IEEE. International Conference on Acoustics, Speech and Signal Processing (ICASSP'91)*, Canada, Apr. 1991, vol. 4, pp. 2557–2560.

[12] B. L. Evans, R. H. Bamberger, and J. H. McCellan, "Rules for multidimensional multirate structures," *IEEE Trans. on Signal Processing*, vol. 42, no. 4, pp. 762–771, Apr 1994.

[13] L.M. Florack, B.M.H. Romeny, J.J. Koenderink, and M.A. Viergever, "Scale and the differential structure of images," *Image and Vision Computing*, vol. 10, no. 6, pp. 376–388, 1992.

[14] T. Lindeberg, *Scale-Space Theory in Computer Vision*, Kluwer Academic, 1994.

[15] T. Lindeberg, "Edge detection and ridge detection with automatic scale selection," in *IEEE Computer Society Conference on Computer Vision and Pattern Recognition (CVPR)*, San Francisco, 1996, pp. 465–470.

[16] Marco Loog and Bram van Ginneken, "Segmentation of the posterior ribs in chest radiographs using iterated contextual pixel classification," *IEEE Trans. Med. Imag.*, vol. 25, no. 5, pp. 602–611, 2006.